AGU PUBLICATIONS

JGR

Journal of Geophysical Research: Oceans

RESEARCH ARTICLE

10.1002/2016JC012106

Key Points:
- The southward freshwater transport north of Denmark Strait between 2011 and 2012 was 65 ± 11 mSv. An additional 19 mSv was present on the shelf
- The shelfbreak EGC carried nearly 70% of the freshwater and the separated EGC was responsible for 30% of the offshore freshwater transport
- The freshwater transport in September 2011 of 131 mSv amounted to an increase with 150% relative to the late-1990s and early-2000s

Correspondence to:
L. de Steur,
Laura.de.Steur@npolar.no

Citation:
de Steur, L., R. S. Pickart, A. Macrander, K. Våge, B. Harden, S. Jónsson, S. Østerhus, and H. Valdimarsson (2017), Liquid freshwater transport estimates from the East Greenland Current based on continuous measurements north of Denmark Strait, *J. Geophys. Res. Oceans*, *122*, doi:10.1002/2016JC012106.

Received 30 JUN 2016
Accepted 21 NOV 2016
Accepted article online 1 DEC 2016

Liquid freshwater transport estimates from the East Greenland Current based on continuous measurements north of Denmark Strait

L. de Steur [1,2], R. S. Pickart [3], A. Macrander[4], K. Våge [5,6], B. Harden [3], S. Jónsson [4,7], S. Østerhus[8], and H. Valdimarsson [4]

[1]Norwegian Polar Institute, Tromsø, Norway, [2]Royal Netherlands Institute for Sea Research (NIOZ), Den Burg, Netherlands, [3]Woods Hole Oceanographic Institution, Woods Hole, Massachusetts, USA, [4]Marine Research Institute, Reykjavík, Iceland, [5]Geophysical Institute, University of Bergen, Bergen, Norway, [6]Bjerknes Centre for Climate Research, Bergen, Norway, [7]School of Business and Science, University of Akureyri, Akureyri, Iceland, [8]Uni Research Climate, Bergen, Norway

Abstract Liquid freshwater transports of the shelfbreak East Greenland Current (EGC) and the separated EGC are determined from mooring records from the Kögur section north of Denmark Strait between August 2011 and July 2012. The 11 month mean freshwater transport (FWT), relative to a salinity of 34.8, was 65 ± 11 mSv to the south. Approximately 70% of this was associated with the shelfbreak EGC and the remaining 30% with the separated EGC. Very large southward FWT ranging from 160 mSv to 120 mSv was observed from September to mid-October 2011 and was foremost due to anomalously low upper-layer salinities. The FWT may, however, be underestimated by approximately 5 mSv due to sampling biases in the upper ocean. The FWT on the Greenland shelf was estimated using additional inshore moorings deployed from 2012 to 2014. While the annual mean ranged from nearly zero during the first year to 18 mSv to the south during the second year, synoptically the FWT on the shelf can be significant. Furthermore, an anomalous event in autumn 2011 caused the shelfbreak EGC to reverse, leading to a large reduction in FWT. This reversed circulation was due to the passage of a large, 100 km wide anticyclone originating upstream from the shelfbreak. The late summer FWT of −131 mSv is 150% larger than earlier estimates based on sections in the late-1990s and early-2000s. This increase is likely the result of enhanced freshwater flux from the Arctic Ocean to the Nordic Seas during the early 2010s.

1. Introduction

The East Greenland Current (EGC) is the main conduit of Arctic freshwater and sea ice from the Arctic Ocean to the subpolar North Atlantic [*Aagaard and Carmack*, 1989]. Anomalous freshwater input to the Nordic Seas and the subpolar North Atlantic can modify surface salinity in convective regions and is therefore thought to play a key role in the overturning strength [*Dickson et al*., 1988; *Manabe and Stouffer*, 1995]. Since the 1990s the freshwater content (FWC) in the Arctic Ocean has increased significantly [*McPhee et al*., 2009; *Rabe et al*., 2014]. In the western Arctic the increase has occurred due to enhanced inputs of sea ice meltwater and river runoff [*Yamamoto-Kawai et al*., 2009], changes in pathways of Eurasian river runoff [*Morison et al*., 2012], and an increase in anticyclonic wind-stress curl leading to convergence of freshwater [*Giles et al*., 2012]. A fresh anomaly was also observed in the Eurasian Basin in 2010 [*Timmermans et al*., 2011] and in the Lincoln Sea between 2007 and 2011, which was suggested to have exited the Arctic through Fram Strait, Nares Strait, or both [*De Steur et al*., 2013]. The fresh anomaly in the Lincoln Sea preceded the return of Pacific Water in Fram Strait in 2011 [*Dodd et al*., 2012] and on the Kögur section north of Denmark Strait near 68°N (Figure 1), between 2011 and 2013 [*De Steur et al*., 2015]. The latter study showed that the amount of Pacific Water in 2013 was as large as the previous maximum measured in 1998 on the same section. In addition, an increase in sea ice melt water has been observed in the EGC in recent years, illustrating the impact of changes in the Arctic Basin on the composition of the freshwater export [*Dodd et al*., 2012; *De Steur et al*., 2015].

Due to seasonal sea ice coverage and the presence of icebergs, as well as the large width of the shelf, the EGC is a difficult region to obtain continuous measurements, hence it is challenging to estimate the

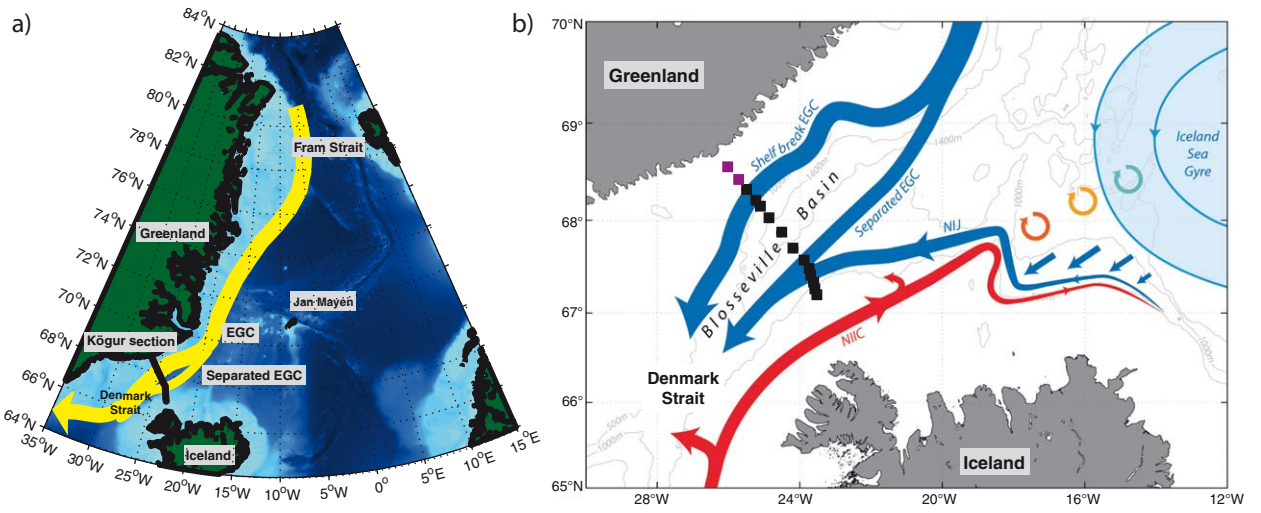

Figure 1. (a) The Nordic Seas with the EGC and separated EGC (both in yellow) and the Kögur mooring array marked northeast of Denmark Strait. (b) A close up of the Kögur region showing a schematic of the southward flowing shelfbreak EGC, the separated EGC and the NIJ (in blue). The northward flowing current (in red) is the North Iceland Irminger Current (NIIC). The mooring array on the Kögur section deployed from 2011 to 2012 is marked with black squares. The purple squares closest to Greenland mark the locations of the two shelf moorings deployed between 2012 and 2014. Figure 1b is adapted from *Våge et al.* [2013] and *Harden et al.* [2016].

freshwater transport (FWT) of the current accurately. The longest record of continuous measurements from the EGC are from the mooring array in Fram Strait. Here the total FWT relative to a salinity of 34.8 was estimated to be close to 130 mSv to the south, of which 62 mSv is liquid freshwater [*De Steur et al.*, 2009] while sea ice volume transport (between 2000 and 2010) was equivalent to 66 mSv of freshwater [*Haine et al.*, 2015]. *Holfort and Meincke* [2005] estimated the liquid freshwater transport of the EGC at 74°N to be 44 mSv, this time relative to 34.9. South of here some fraction of the freshwater is diverted into the interior Nordic Seas: approximately 10 mSv flows eastward with the Jan Mayen Current [*Dickson et al.*, 2007], while 3.4 mSv is carried southeastward with the East Icelandic Current [*Macrander et al.*, 2014]. Furthermore, a significant amount of sea ice is believed to escape into the interior with an equivalent of 49 mSv of freshwater [*Dodd et al.*, 2009]. Still farther south, between the Kögur section and Cape Farewell (southern tip of Greenland), the equatorward FWT was shown to increase from 59 mSv to 96 mSv (relative to a salinity of 34.8) based on summertime shipboard data [*Sutherland and Pickart*, 2008]. This southward increase could be explained by inputs from sea ice and iceberg melt, runoff and net precipitation. The first two inputs are obviously largest in summer, and, due to the synoptic nature of these latter estimates they should be interpreted with care.

Upstream of Denmark Strait, near the northern end of the Blosseville Basin, the EGC bifurcates [*Våge et al.*, 2013] (Figure 1). This was deduced using four occupations of the Kögur section between 2004 and 2012, together with a numerical model. The offshore branch is referred to as the separated EGC and, like the shelfbreak EGC, is a surface-intensified, southward-flowing jet. It is known to meander, but is a year-round feature [*Harden et al.*, 2016]. Based on the four occupations of the Kögur section used in *Våge et al.* [2013], the summertime mean FWT was estimated to be 159± 28 mSv in absence of sea ice. While the bulk of the freshwater was advected by the shelfbreak EGC, almost 25% of the total FWT was associated with the separated EGC [*Våge et al.*, 2013]. The exact formation mechanism of the separated EGC is still a subject under investigation; both the negative wind-stress curl over the Blosseville Basin as well as the change in orientation of the Greenland coast relative to the dominant wind direction at 69°N appear to play a role [*Våge et al.*, 2013]. Regardless of the precise mechanism(s), however, it is clear that the separated EGC is important for transporting freshwater away from the shelfbreak into the interior. Hence, in order to quantify the total southward FWT of the EGC into the subpolar gyre, one must sample the full distance between Greenland and Iceland at this latitude.

Between 2011 and 2012 an array of 12 full-depth moorings was deployed across the Kögur section (Figure 1) in order to study the complex current system consisting of the shelfbreak EGC, separated EGC, and the North Icelandic Jet (NIJ), a deep and dense southward jet along the Iceland continental slope [*Jónsson and*

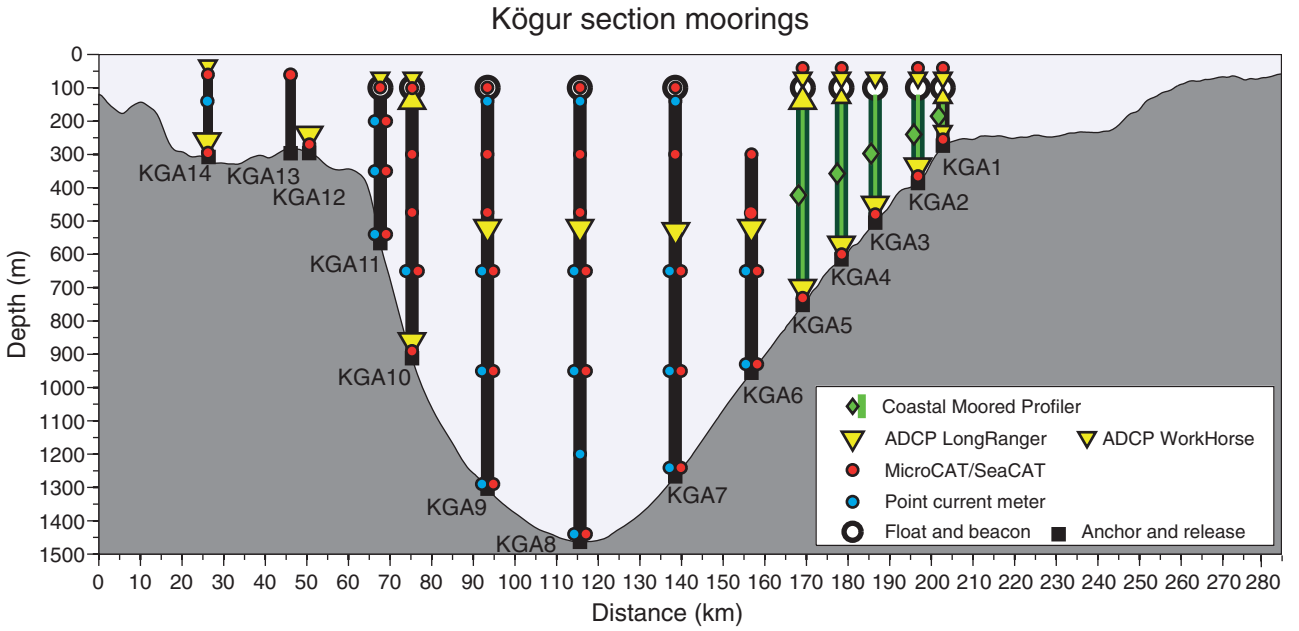

Figure 2. Cross section of the Kögur mooring array with moorings KGA1 through KGA12 from east to west for the main deployment period 2011–2012. Instruments that were lost from the top of KGA3 and KGA6 are excluded from the figure. Moorings KGA12, KGA13 and KGA14 on the east Greenland shelf were deployed from August 2012 to July 2014.

Valdimarsson, 2004]. The array provided the first high-resolution continuous measurements of temperature, salinity, and velocity of this region. *Harden et al.* [2016] have used these data to quantify the transport, variability, and relative contributions of the EGC (both branches) and NIJ to the Denmark Strait Overflow Water. In this paper we use the same data set, in conjunction with shipboard hydrographic data from the region, to quantify the year-round FWT and investigate the variability of the FWT in the total EGC system. In addition, data from two shallow moorings that were deployed on the east Greenland shelf between 2012 and 2014 are incorporated to obtain estimates of the FWT inshore of the shelfbreak. The outline of the paper is as follows. The data and methods are presented in section 2. The results of the freshwater transports at the main Kögur section between 2011 and 2012, as well as an analysis of two shelf moorings between 2012 and 2014, are given in section 3. The relationship between the wind forcing, sea-surface height and the observed FWT variability is also explored here. The discussion follows in section 4 and the conclusions are given in section 5.

2. Data and Methods

We use data from an array of 12 moorings deployed along the Kögur section from late August 2011 until July 2012 (Figure 1). Three moorings covered the east Greenland outer-shelf and slope (KGA10–KGA12), four moorings spanned the central/deep part of the section (KGA6–KGA9), and five moorings sampled the NIJ on the Iceland slope (KGA1–KGA5) (Figure 2). Distance along the mooring section is positive from the east coast of Greenland. The moored instruments consisted of RDI acoustic Doppler current profilers (ADCPs, both 75 kHz and 150 kHz), Nortek Aquadopps, Aanderaa Recording Current Meters (RCM9 and RCM11), Aanderaa Recording Doppler Current Profiler (RDCP-600), and SBE37-SM MicroCATs. The moorings in the NIJ were equipped with Coastal Moored Profilers (CMPs) providing vertical profiles of temperature and salinity. The shallowest MicroCATs were located at 50 dbar. Velocity data (V) were obtained at 1 h or 20 min intervals, and point temperature/salinity (T/S) measurements were made at 15 min intervals (data were not averaged over the interval periods). The CMPs profiled three times daily. The velocity data were low-passed with a 40 h filter to remove tides. V and S were then averaged to get daily mean values.

The overall data return on the array was approximately 95%, which is exceptionally high considering the presence of icebergs in the western part of the domain as well as intense fishing activity through much of the region. Only a few of instruments were lost or failed during the deployment period. On KGA3 the top MicroCAT at 50 m was lost, as well as a MicroCAT and current meter at 100 m depth at KGA6 (probably due to trawling). The latter caused the MicroCAT at 300 m to drop to roughly 650 m depth after 100 days. The

upward looking ADCP at KGA10 had a compass failure; however, the velocity data were subsequently corrected by using the compass direction of the downward looking ADCP just below it (see *Harden et al*. [2016] for more details). Unfortunately the downward looking ADCP on that mooring also stopped working in April 2012, leaving a data gap of 3 months. In addition, the ADCPs at the bottom of KGA2 and KGA5 stopped 1 month prematurely.

As part of a pilot study on FWT on the Greenland shelf, KGA12 and two additional moorings, KGA13 and KGA14, were deployed from August 2012 to July 2014. During these 2 years there were also some instrument failures on KGA14: the single point current meter failed during the 2012–2013 deployment, and the two ADCPs stopped after 2 months during the 2013–2014 deployment.

2.1. Addressing Data Gaps in the Time Series

In order to quantify the total FWT across the Kögur section, consistent data matrices of S and V–in space and time–are made. As such, the data gaps caused by instruments that stopped prematurely or that were lost are filled before interpolation.

At the locations where salinity and/or velocity data are missing for a period of time, and for near-surface bins of ADCPs with low quality velocity data, the gaps were filled through a linear regression with time series of instruments nearby or velocity data at greater depth. The optimal instrument and time series from which to determine regression coefficients were identified by finding the largest correlation between time series before an instrument stopped or was lost. Generally the best correlation for V was found in the vertical. Using mooring KGA10 as an example, an extended time series was constructed according to

$$V_{KGA10}(z_i) = b_0 + b_1 . V_{KGA10}(z_{i+1}) \tag{1}$$

where V_{KGA10} is the velocity at mooring KGA10, z_i is the depth level of the instrument, and $b_{0,1}$ are the coefficients determined by linear regression when time series were available at both levels z_i and z_{i+1}. In the case of S the best correlation between time series was more often found in the horizontal, though not always. Using KGA10 and KGA11 as examples, an extended time series of S was constructed either following equation (1) or according to

$$S_{KGA10}(z_i) = b_0 + b_1 . S_{KGA11}(z_i) \tag{2}$$

Since there was no salinity sensor in the upper ocean at KGA12, artificial time series of S at that site at 50 m and 100 m depth were obtained in a similar way through regression of time series of S at 300 m between KGA12 and KGA11. This approach is justified since data from the two shelf moorings during 2012–2014 showed very good correlation between S at those depths. A sensitivity test was carried out to see how robust this method of dealing with data gaps is. This was done by artificially withholding more data sets from the array and computing the transports again using the same protocols for regression, interpolation and extrapolation. The differences obtained were on the order of just 2 mSv for FWT and 0.1 Sv for volume transport. This shows that the method used is robust.

2.2. Upper Ocean Stratification

To obtain realistic surface layer stratification for S above the uppermost moored instruments, hydrographic data obtained during the deployment and recovery cruises in 2011 and 2012, together with climatological hydrographic data, were incorporated. As seen in Figure 2, the near-surface instrumentation of the Kögur array was limited to approximately 50 m or 100 m below the surface. Since upper ocean salinity in the EGC is influenced by freezing and melting of sea ice – and hence very stratified in summer – it is not straightforward to obtain appropriate near-surface values via simple extrapolation. One approach is to use optimal interpolation, which was implemented in *Harden et al*. [2016]. Here we make use of all available hydrographic data from 2002 to 2014 in the region between 66.4°N−68.73°N and 20°W−30°W. The data include the four above-mentioned summer occupations of the Kögur section carried out between 2011 and 2014 [*Våge et al*., 2013], spring data from the 2002 Oden cruise AO-02 [*Nilsson et al*., 2008], year-round profiles collected by instrumented seals during the IPY 2007–2008 [*Isachsen et al*., 2014], and all other available profiles obtained from the ICES hydrographic data base (www.ices.dk).

The amount of ship-based hydrographic winter and spring data from the region is very limited due to the sea ice cover during that time of year. However, sensors attached to hooded seals during the IPY (2007–

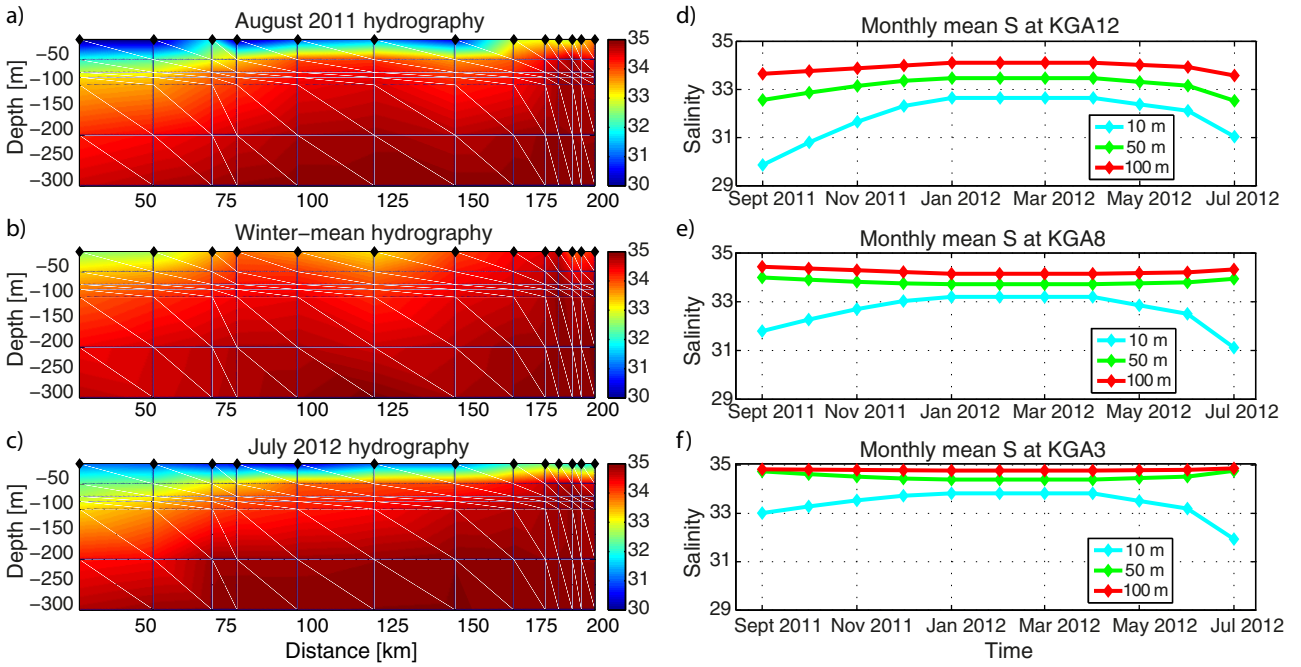

Figure 3. Cross sections of salinity on the Kögur section for (a) August 2011, (b) winter-mean hydrography based on all available winter data in the 2000s, and (c) July 2012. The mooring positions are marked by black diamonds. Monthly mean salinity at 10 m, 50 m, and 100 at mooring sites (d) KGA12, (e) KGA8, and (f) KGA3.

2008) provided a considerable amount of temperature and salinity profiles from February, March, and April from the Nordic Seas. Earlier mooring records from 74°N have shown that the upper ocean salinity in the EGC is mostly determined by a large seasonal cycle related to freeze up and melting of sea ice and is therefore strongly correlated with sea ice cover [*Holfort and Meincke*, 2005]. The associated change in salinity between March and September at a nominal depth of 20 m was shown to be as much as 3.5–4 salinity units, while at a depth of 60 m it was 1–1.5 salinity units. Inspection of the summertime shipboard hydrographic data and the wintertime seal data projected onto the Kögur section show a similiar result (Figures 3a–3c). To obtain a seasonal cycle of S at depths of 10 m, 50 m, and 100 m across the array, sinusoidal curves were fit through the summer and winter near-surface hydrographic data (Figures 3d–3f). This seasonal cycle of the upper-ocean stratification constructed from hydrographic data at selected depths was then used to construct time series at 10, 50, and 100 m using the relationship between the time series from the top-most instrument at each mooring site and the upper-ocean stratification. Finally, S above 10 m is assumed to be constant from 10 m depth to the surface.

The daily data at the instrument locations, and the synthetic time series at the upper levels, were subsequently linearly interpolated in the vertical at 5 m intervals above 150 m depth, and on (nonequidistant) intervals parallel to the bottom below 150 m depth (i.e., vertical spacing varying between 10 and 85 m). Following this the data were objectively interpolated in the horizontal with approximately 1 km resolution. Finally, the FWT across the mooring section was determined according to

$$FWT = \int_{x=50}^{x=210} \int_{z(S=S_{ref})}^{z=0} V_{\perp}(x,z) \cdot \frac{S_{ref} - S(x,z)}{S_{ref}} \, dz \, dx \tag{3}$$

where $V_{\perp}$ is the velocity component normal to the section and S_{ref} the reference salinity. $V_{\perp}$ is defined positive to the northeast and errors are of the order 1 cms^{-1}. In general we show results for S_{ref} =34.8, but we also include estimates based on S_{ref} =34.9 in order to compare with previously published values. The sensitivity of the FWT to a reference salinity of 34.8 or 34.9 is, however, small. The FWT is integrated in the horizontal between 50 and 210 km distance on the section and in the vertical between the surface and the depth of the isohaline $S_{ref.}$ The upper boundary of the integral is the surface, however, one should keep in mind that both S and V are assumed constant between 10 m and the surface. Hence, we likely underestimate the FWT by about 5 mSv.

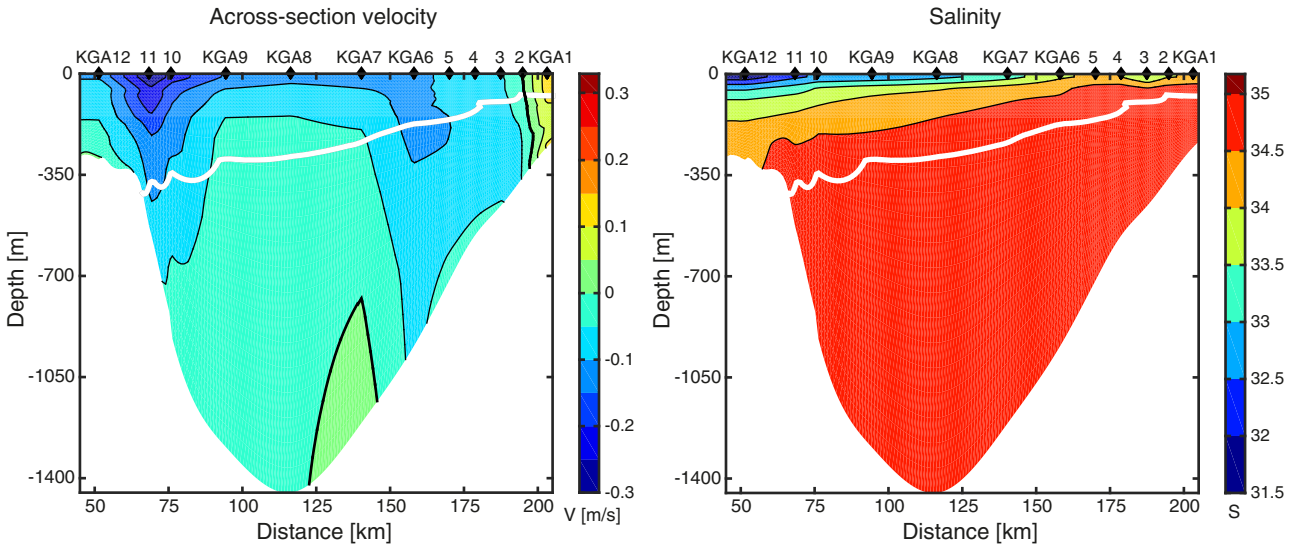

Figure 4. Cross sections of 11 month mean across-section velocity (left) $V_\perp$ and (right) S on the Kögur section based on interpolated mooring data. $V_\perp$ is negative to the south. The white contour marks the 11 month mean location of the 34.8 isohaline. Contour intervals are 0.05 m s^{-1} for V and 0.5 for salinity. The mooring sites are marked at the top of the sections.

Following *Jahn et al.* [2012], the FWT is split into a time-mean component and three time-varying terms which are related to (i) anomalies in the freshwater concentration $C_{FW} = \int_{x=50}^{x=210} \int_{z(S=34.8)}^{z=10} \frac{S_{ref} - S(x,z)}{S_{ref}}$ (which basically reflect anomalies in S); (ii) anomalies in $V_\perp$; and (iii) a combination of the two according to

$$FWT = \langle C_{FW} \rangle \langle V_\perp \rangle + V'_\perp \langle C_{FW} \rangle + C'_{FW} \langle V_\perp \rangle + C'_{FW} V'_\perp \quad (4)$$

where brackets $\langle\,\rangle$ indicate the time mean, and primed variables $'$ indicate temporal anomalies.

3. Results

The 11 month mean $V_\perp$ and S fields on the mooring section are shown in Figure 4. The mean location of the 34.8 isohaline is marked by the white contour. The mean velocity field shows the distinct shelfbreak EGC on the east Greenland continental slope, centered at mooring KGA11. On the Iceland slope the signature of enhanced equatorward flow is due to a combination of the separated branch of the EGC and the NIJ, which are in the process of merging at this location [see *Harden et al.*, 2016]. Note that at mooring KGA6 the southward flow is surface-intensified (indicative of the separated EGC), whereas at mooring KGA5 the flow is middepth intensified (characteristic of the NIJ). As discussed in *Harden et al.* [2016], at times the two currents are distinct, but in the mean they appear merged. To the east, near the Iceland shelfbreak, the poleward-flowing North Icelandic Irminger Current is visible. The mean salinity field shows the freshest water on the Greenland shelf in the west, while east of the shelfbreak EGC there is a gradual transition to less fresh surface waters.

Monthly mean velocities and salinities between September 2011 and July 2012 are shown in separate panels (Figures 5 and 6). Generally the shelfbreak and the separated branches of the EGC are visible in all months, although the latter varies substantially both in location and strength. The shelfbreak EGC also varies in strength with maximum velocities and a deeper-reaching core in the winter months. The most striking event in the flow field occurred in November when a large anticyclonic feature occupied nearly the entire section, with strong northward flow on the east Greenland slope and anomalously strong and deep southward flow on the Iceland slope. Either the shelfbreak EGC was pushed farther west onto the shelf (beyond the westernmost mooring) or it was fully separated from the shelfbreak at this time such that all of the EGC waters were transported by a strengthened separated branch.

Since the time series were only 11 months long, the mean V is likely on the low side relative to an annual mean (since weakest V occurs in summer). The 11 month mean S is likely higher than an annual mean since the month of August that was not covered by the deployment would have contributed with very low

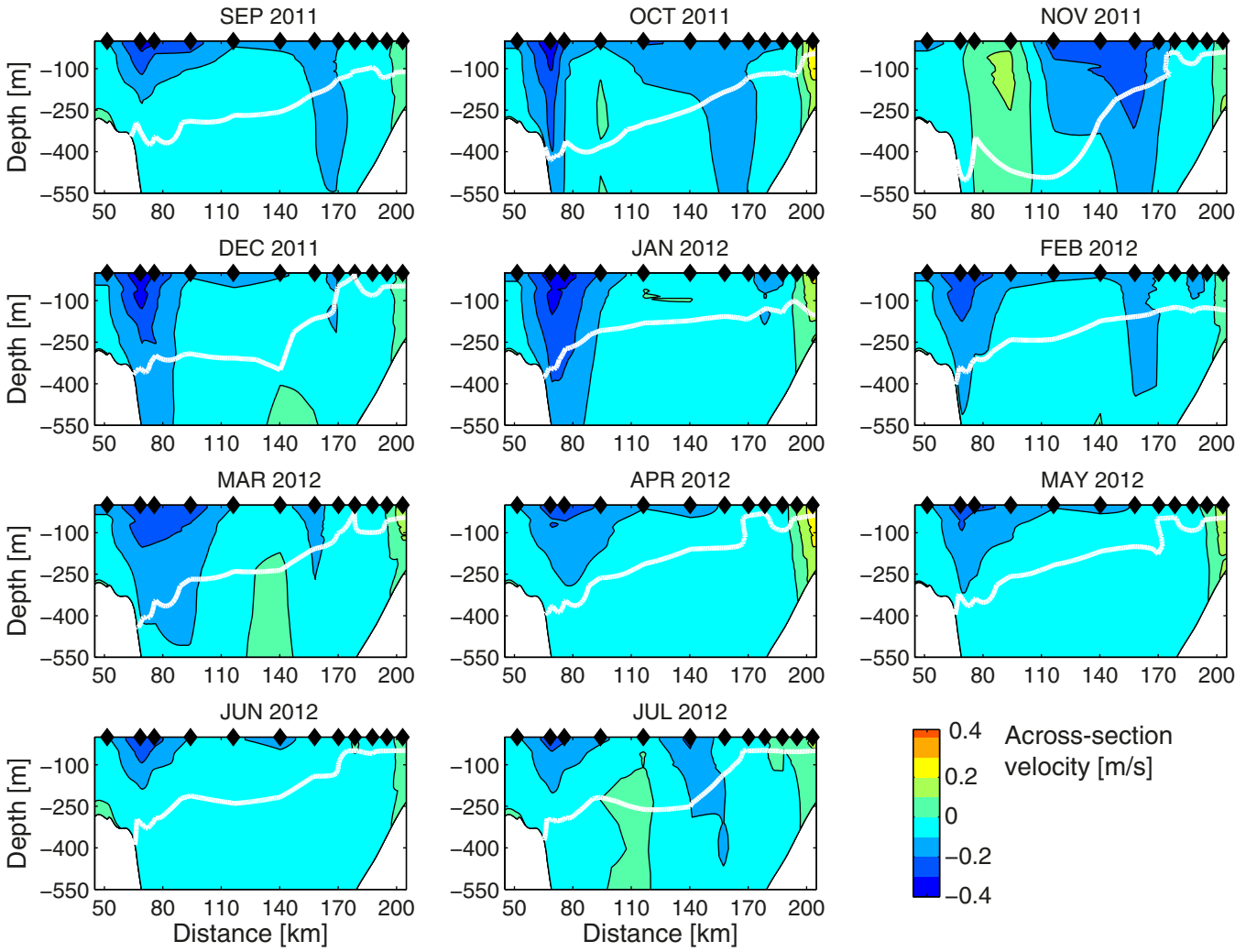

Figure 5. Monthly mean cross sections of $V_\perp$ on the Kögur section based on interpolated mooring data. The white contour marks the monthly mean location of the 34.8 isohaline. The mooring sites are marked at the top of the sections.

surface S due to enhanced melt and runoff. Hence, a full annual mean freshwater transport would likely be larger than our estimate based on 11 months.

3.1. Freshwater Transport by the Two Branches of the EGC

The total five-day low passed and monthly mean FWT are calculated for the section between 50 and 210 km (Figure 7a) where negative values indicate southward flux. Here we present transports for S_{ref} =34.8, but the values for S_{ref} =34.9 are given in parentheses. The largest southward FWT occurred in September and October, with values up to −169 mSv (−179 mSv). Minimum southward FWT occurred in November when the net transport was nearly zero; this was due to the strong flow reversal on the Greenland slope leading to a northward FWT over that part of the section. The 11 month mean FWT excluding the Greenland shelf was −65 mSv (−74 mSv) with a standard deviation of 30 mSv. The standard error (standard deviation/$\sqrt{n}$) associated with the mean value obtained from a number of independent samples (n), however, is much smaller. The time series consists of 332 daily values and we determined the time series to have a decorrelation time scale τ of 3 days. This implies that the number of uncorrelated samples is 332/$2\tau = 55$ such that the standard error is 30 mSv/$\sqrt{55}$ which is close to 4 mSv. However, perhaps more relevant is the error estimate for each daily mean FWT value related to propagating individual errors of V (0.01 m/s), S (0.5, considering the seasonal cycle that was constructed on relatively sparse winter data in the uppermost 50 m), and the uncertainty related with gridding the data (200 m in the horizontal and 2 m in the vertical) into the daily FWT calculations. The mean of those daily obtained error estimates was

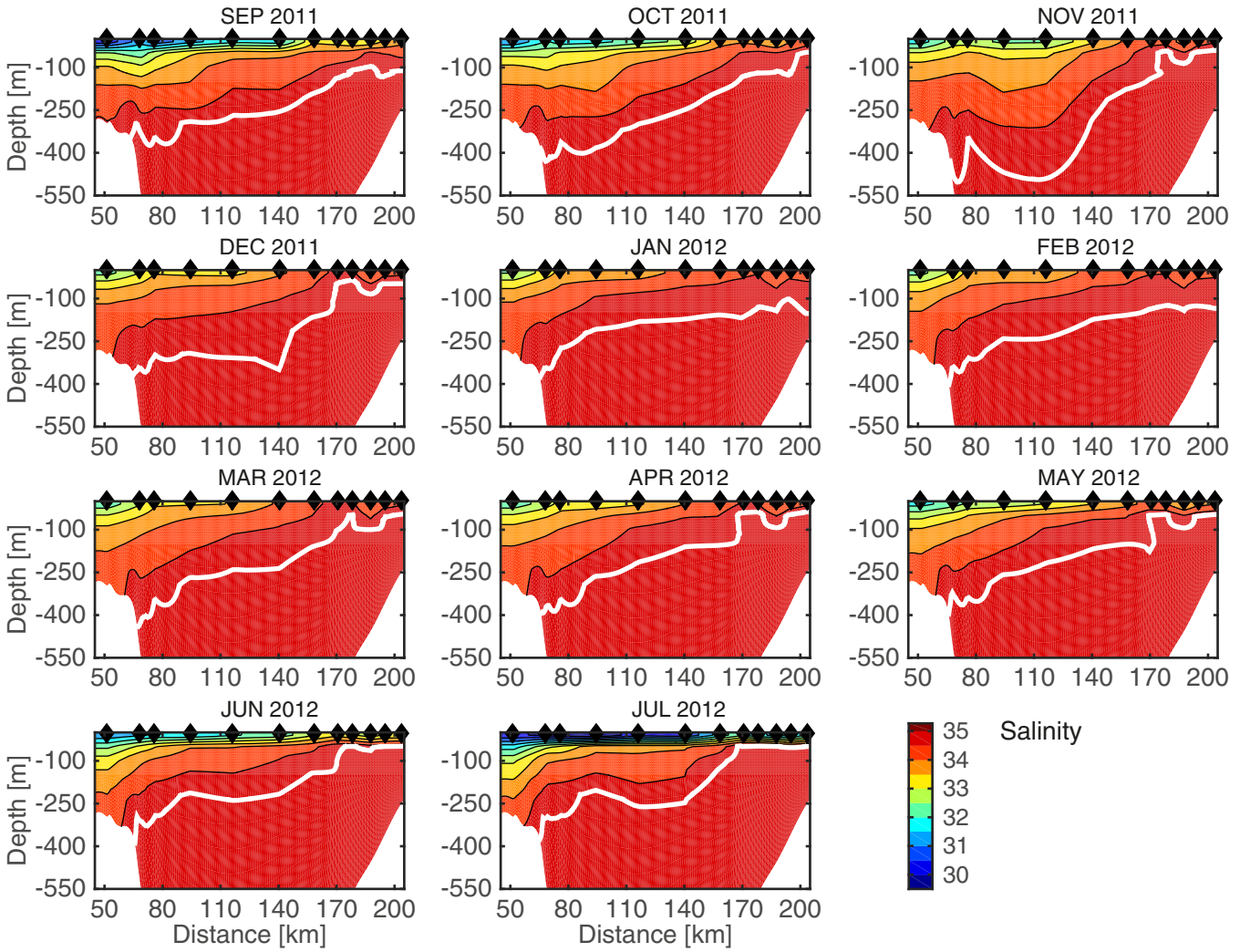

Figure 6. Same as Figure 5 except for *S*.

11 mSv for the choice of the individual errors. We therefore take this latter value as the error associated with the mean FWT estimate.

The separation of FWT anomalies into contributions related to velocity and salt anomalies (according to equation (4)) shows that both terms are important throughout the period (Figure 7b). While the flux term dominates the FWT in November, the salt term shows a seasonal cycle with maximum contribution in late-summer and minimum contribution in winter when brine dominates over melt.

Figure 5 shows that the boundary between the shelfbreak and separated EGC was quite variable in time. In order to distinguish and quantify the FWT of the two branches separately, the absolute minimum in velocity at 50 m depth was determined between 75 and 125 km distance on the section each day. This was taken as the boundary between the two currents. Furthermore, the separated EGC and the NIJ were distinguished from each other by using the same dynamic boundary between the EGC and the NIJ as *Harden et al*. [2016], which is based on a quantitative end-member analysis of the water masses carried by each current. As seen in Figure 8, the shelfbreak EGC dominated the total FWT apart from the months October and November. Peak values of the 5 day low passed shelfbreak and separated EGC FWT were up to −160 mSv (−169 mSv) and −88 mSv (−99 mSv), respectively. The 11 month mean values of FWT for the shelfbreak EGC and the separated EGC were −47 mSv (−52 mSv) and −16 mSv (−18 mSv), respectively. The extrema in FWT of the NIJ were −10 mSv (−16 mSv) and +10 mSv (10 mSv), while the 11 month mean FWT was only −2 mSv (−3 mSv). The mean FWT estimates for the different branches and for different reference salinities are

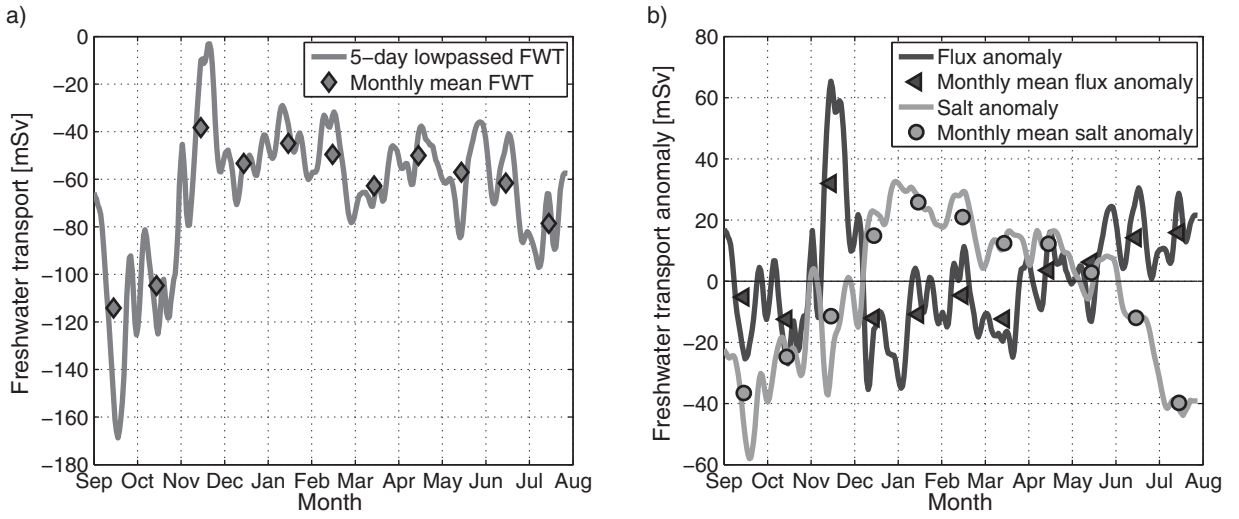

Figure 7. (a) Five day low-pass filtered daily and monthly mean FWT on the Kögur section between September 2011 and July 2012. (b) Five day low-pass filtered daily and monthly mean values of the flux anomaly and salt anomaly terms of the total FWT.

summarized in Table 1. The velocity, salt and cross terms of equation (4) were also calculated for each branch separately (not shown). For both branches the contributions of velocity and salt anomalies were of roughly of equal importance during the period. While the salt term showed a slowly seasonally varying signal in each case, the velocity term was more variable throughout the year and it dominated the anomalous northward FWT of the shelfbreak EGC in November. Also, the cross term (term 4 in equation (4)) was not negligible during November when the flow reversal took place over the east Greenland slope.

In addition to the FWT we present the upper ocean volume transport of the East Greenland Current (i.e., low density) Arctic water (Figure 8b and Table 1). This is defined as water $\sigma_\theta < 27.8\,\mathrm{kg\,m^{-3}}$. The dense contributions, forming the sources of the DSOW at Denmark Strait, have been presented in *Harden et al.* [2016]. We find that the volume transport of the upper ocean ($\sigma_\theta < 27.8\,\mathrm{kg\,m^{-3}}$) across the Kögur section was -1.78 Sv $\pm$ 0.63 Sv standard deviation of the daily mean values, a standard error of 0.1 Sv, and mean error related to gridding of 0.45 Sv. Largest southward transport occurred in autumn and winter and weakest transport in summer (apart from the anomalous flow reversal in November (see section 4)) and the

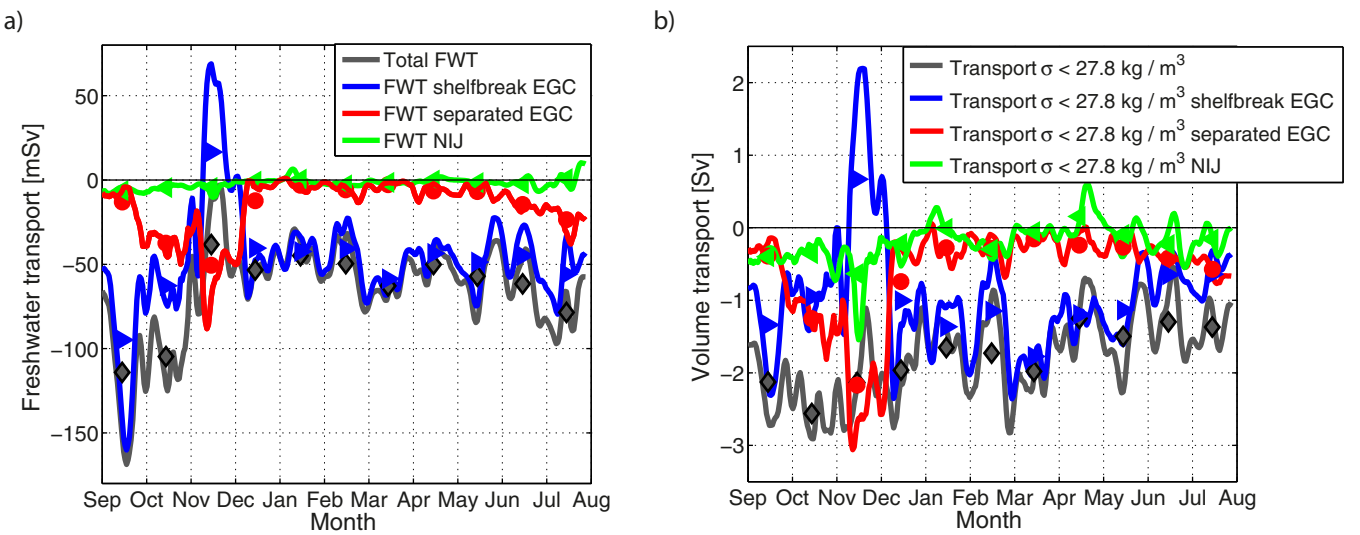

Figure 8. (a) Five day low-pass filtered daily means of total FWT on the section, the FWT of the shelfbreak EGC, and the separated EGC. The symbols (diamonds, squares and circles) mark the monthly mean values. (b) Five day low-passed total volume transport of upper ocean water with S<34.65 (the equivalent of $\sigma_\theta < 27.8\,\mathrm{kg\,m^{-3}}$), and that of the shelfbreak and separated EGC as well as the NIJ.

Table 1. FWT and Volume Transport for Different Values of S_{ref} Between 2011 and 2012

FWT Relative to S_{ref}	Total	Greenland Shelf	Shelfbreak EGC	Separated EGC	NIJ
34.65	−71 mSv	−17 mSv	−40 mSv	−13 mSv	−1 mSv
34.8	−84 mSv	−19 mSv	−47 mSv	−16 mSv	−2 mSv
34.9	−94 mSv	−20 mSv	−52 mSv	−18 mSv	−3 mSv
Volume transport for $S<S_{ref}$	**Total**	**Greenland shelf**	**Shelfbreak EGC**	**Separated EGC**	**NIJ**
34.65	−2.72 Sv	−0.46 Sv	−1.50 Sv	−0.63 Sv	−0.13 Sv
34.8	−3.28 Sv	−0.46 Sv	−1.77 Sv	−0.79 Sv	−0.27 Sv
34.9	−4.84 Sv	−0.46 Sv	−2.15 Sv	−1.13 Sv	−1.12 Sv

[a]The estimate for the Greenland shelf is obtained by regression of time series at KGA12 with KGA13 and KGA14 in 2012–2014.

difference could be up to 1 Sv. Between 2011 and 2012 the shelfbreak EGC transported on average 1 Sv while the separated EGC and the NIJ together transported nearly 0.8 Sv of low-density water. The dense volume transports with $\sigma_\theta > 27.8\,\mathrm{kg\,m^{-3}}$ of the shelfbreak EGC and the separated EGC across the Kögur section, amounted to 1.50 Sv and 1.04 Sv, respectively (or 60% versus 40% of the total dense transport) [*Harden et al*., 2016]. However, when the Greenland shelf (west of 50 km distance) is taken into account, another 0.45 Sv needs to be added to the upper ocean (low-density) transport. And the contributions of the low and high-density water to the EGC system above sill depth are comparable. The shelf is also significant for the net FWT as will be shown in the next section.

3.2. Freshwater Transport on the East Greenland Shelf

The above estimate of FWT from the mooring array did not include the Greenland shelf west of 50 km, and therefore a potentially significant portion of the FWT was not captured. The two additional shelf moorings KGA13 and KGA14 that were deployed between 2012 and 2014, in addition to a redeployment of KGA12, allow for a first estimate of the year-round transport on the shelf. Moorings KGA12 and KGA13 were deployed in tandem to obtain near-bottom and near-surface salinity measurements on the outer shelf, while KGA14 was deployed roughly 25 km inshore of this (also with shallow and deep salinity measurements, see Figure 2). Note, however, that there is still a 25 km gap between KGA14 and the coast and that the FWT on the shelf is therefore probably still underestimated. To produce this value we used the same approach as discussed in section 2.2 to account for data gaps and to include upper-ocean stratification.

The shelf FWT calculated as such was highly variable (Figure 9) which was mostly related to variations in the flow. While the 5 day low-passed values ranged from −59 mSv (−62 mSv) to +85 mSv (+87 mSv), the annual mean FWT on the shelf was only −1 mSv (−1 mSv) between 2012 and 2013. Again, these are relative to S_{ref} =34.8 while the numbers in parentheses indicate the FWT relative to 34.9. Between 2013 and

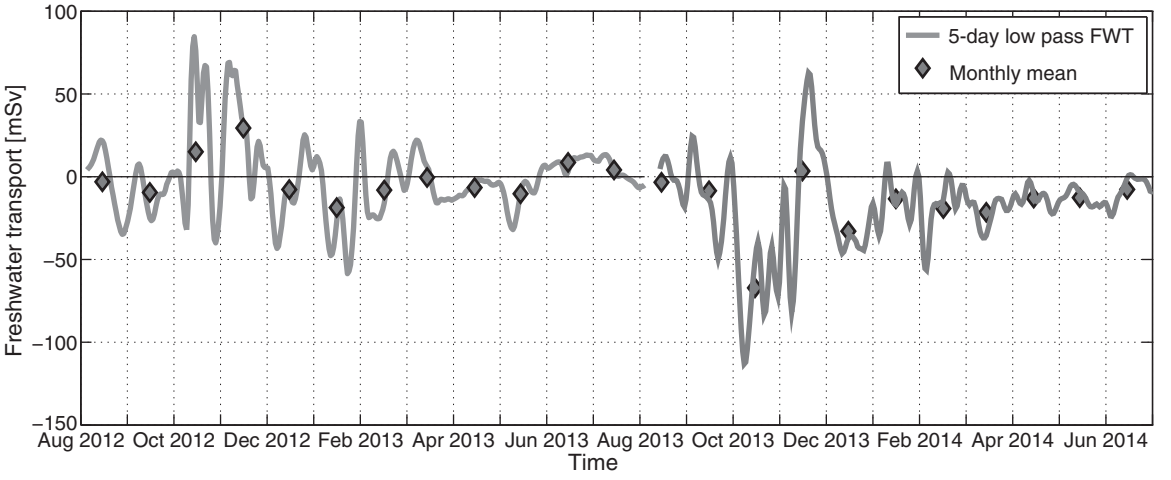

Figure 9. Five day low-pass filtered and monthly mean values of FWT on the shelf based on two moorings between 25 and 50 km from the Greenland coast.

2014 the annual mean was −18 mSv (−19 mSv) with daily peak values of −113 mSv (−117 mSv) and 63 mSv (65 mSv). These results illustrate that the FWT on the shelf is extremely variable in time and can contribute substantially to the net FWT across the section. One sees in Figure 9 that the fluctuations have the highest amplitude during the fall and early-winter, which may be related to the sea ice. In particular, it has been shown that for partial ice cover – during the period of freeze-up – the transfer of momentum into the ocean from the wind is enhanced due to the ice-ocean stress via the mobile ice pack [*Schulze and Pickart*, 2012; *Pickart et al*., 2013]. Furthermore, storms in the region are most intense at this time of year.

We used the information obtained from the shelf moorings in 2012–2014, in particular the regression coefficients for the velocities and salinities at KGA12 and KGA14, to extend the FWT record on the shelf back in time for the 2011–2012 deployment. The time series of S at the two shelf sites are significantly correlated both for the shallow level (correlation coefficient of 0.80) and the near-bottom level (0.54). In addition, V is correlated at the shallow level (0.51), where the FWT is largest. While there was no correlation between the time series of V at the bottom of KGA12 and KGA14, the velocities at depth on the shelf were found to be relatively small ($<\pm 0.12\,\mathrm{m\,s^{-1}}$). Using these regressions we estimate an annual mean FWT of −19 mSv (−20 mSv) for 2011–2012 (the associated error is per definition larger than that for the 2012–2014 value). We note that the large variability observed in the autumn of 2012 and 2013 is not captured using this technique, since the extreme flow variations occurred predominantly at mooring site KGA14. Furthermore, compared with the FWT estimates from the hydrographic sections in summers 2011 and 2012 [*Våge et al*., 2013], the estimate from the shelf moorings appears to be biased low. Therefore, we conclude that there was a substantial FWT on the shelf during 2011–2012 and the estimate of −19 msv is likely a lower bound.

3.3. Anomalies in FWT

Very large southward FWTs in were observed in September 2011, October 2011, and July 2012. These large FWTs were predominantly due to large anomalies in salinity adding −40 mSv in the montly mean (Figure 7b). In 2011, the velocity anomaly was also negative (i.e., enhanced southward flow) leading to exceptionally large southward FWT while in July 2012 the velocity anomaly relative to the mean was positive. Closer inspection of salinity data from hydrographic sections from 2004, 2008, and between 2011 and 2013 shows that the mean salinity between 0 and 40 m across the Kögur section (between 0 and 200 km) was in fact one whole salinity unit lower in 2011 (S=30.7) than the mean between 2004 and 2013 (S=31.7). Particularly the mean upper ocean salinity on the shelf was 1.2 salinity units lower in 2011 (S=30.3) than the mean of the 5 years mentioned above (mean S=31.5). The magnitude of this salinity anomaly in 2011 is of similar magnitude as the upper ocean salinity anomaly seen in the early 1990s during which a large amount of liquid FW was released from the Arctic [*Karcher et al*., 2005]. The fresh event in 2011, however, was not associated with particular low salinities below 40 m. When considering the upper 200 m (section wide), then 2013 was actually freshest of the other years considered. We discuss this further in Section 4.

We now explore the anomalous event in November 2011 (Figures 5 and 7b) during which the FWT and volume transport of the shelfbreak EGC were reversed, while the corresponding transports of the separated EGC were exceptionally strong to the south. One explanation for the separated EGC involves the negative wind-stress curl over closed isobaths in the Blosseville Basin, which can set up a local anticyclonic gyre (the southward branch being the separated EGC) *Våge et al*. [2013]. This was further investigated by *Harden et al*. [2016] to help explain variability in the partitioning of dense overflow water ($\sigma_\theta < 27.8\,\mathrm{kg\,m^{-3}}$) between the shelfbreak EGC and separated EGC. It was shown that fluctuations in the transport of overflow water in the two branches were out of phase on time scales longer than 20 days, and that this was weakly correlated with the wind-stress curl across the array. This mechanism can explain the stronger deep flow observed on the Greenland side of the Kögur section in winter (see panels for December through March in Figure 5) when positive wind-stress curl dominated.

While *Harden et al*. [2016] focused on the overflow layer, here we are considering the upper layer corresponding to $S < 34.8$ and find that the event in November cannot be explained by wind-stress curl alone. To demonstrate this we constructed a time series of average wind-stress curl averaged over the area bounded by the 1400 m bathymetric contour defining the Blosseville Basin (Figure 10), using the North American Regional Reanalysis (NARR) wind product [*Mesinger et al*., 2006]. The two-week lowpass of this is shown in relation to the volume transport of the separated EGC ($S < 34.8$, similarly low-passed) in Figure 10. The wind-stress curl was mostly positive during the first 6 weeks of the deployment period (up to mid-October). Thereafter it was strongly negative for a period of almost three weeks, followed by a weakening (though still

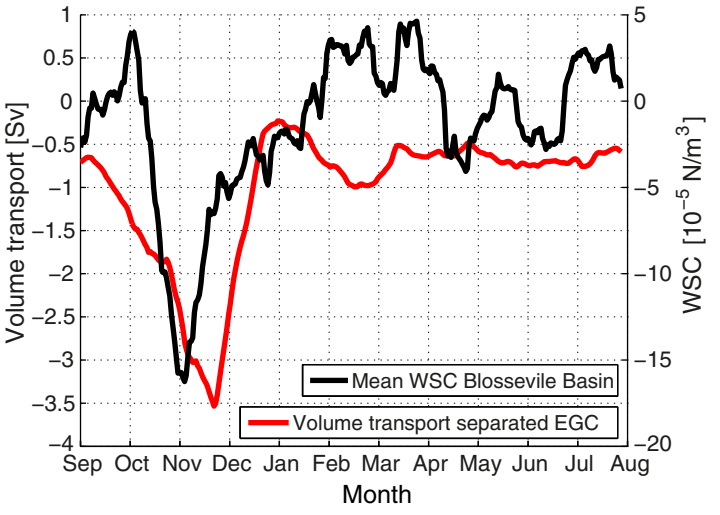

Figure 10. Two week low-pass filtered values of the volume transport of the separated EGC and the mean daily-mean wind-stress curl averaged over the Blosseville Basin where isobaths are greater than 1400 m.

negative) for another month. Between January 2012 and early April 2012 the wind-stress curl was generally positive (which was responsible for the stronger deep flow seen in the shelfbreak EGC during that time [*Harden et al.*, 2016]). After this the curl alternated between weakly positive and negative values until the end of the record. Notably, the southward transport of the separated EGC increased substantially during September, even though the wind-stress curl was near-zero or positive during that month. Furthermore, the maximum equatorward transport of the separated EGC during the November event occured nearly 3 weeks after the peak in negative wind-stress curl over the Blosseville Basin. Both of these things imply that wind-stress curl was not the sole driver of the event.

To investigate this further we considered the delayed-time Level 4 Sea-Level Anomaly (SLA) product (Ssalto/Duacs obtained from AVISO). Panels of SLA north of Denmark Strait are shown every 5th day between 4 November and 14 December 2011 (Figure 11). Inspection of sea ice concentration maps [*Cavalieri et al.*, 1996] shows that in October the formation of sea ice begins on the shelf near Greenland, continuing into November when sea ice concentration starts to increase. As of January 2012 the western half of the section is nearly 100% sea-ice covered and is therefore not included. For reference, the contour marking 80% sea ice concentration is shown in Figure 11. On 4 November two large areas with positive SLA were visible offshore of Greenland. Of particular note is the isolated feature situated over the shelf and slope northeast of the Kögur section. The consecutive panels show that this feature moved toward the section while its maximum SLA expression decreased slowly. At the same time the center of the feature gradually shifted downslope and reached the middle of the Kögur section between 14 and 19 November. It continued this equatorward progression until it was south of the array by early December.

Such an isolated feature with positive SLA is likely a large anticyclonic eddy. Indeed, Hovmöller diagrams of SLA and upper-ocean velocity (at 60 m depth) across the array demonstrate that the timing of the eddy, as well as its size (over 100 km), corresponds well with the anticyclonic circulation measured at the mooring array in mid-November (Figure 12). Note that the reversed circulation during this event did not coincide with positive wind-stress curl over the Blosseville basin (Figure 10). Thus it is clear that the passage of mesoscale features in this region can significantly modify the volume transport and FWT of both the shelfbreak and separated EGC.

4. Discussion

It is of interest to compare our mooring-based estimates of FWT at the Kögur section to values derived from shipboard occuptions of the line. The monthly mean FWT of the separated EGC in September 2011 and July 2012 calculated from the mooring records were −13 mSv and −24 mSv, respectively. These values are in agreement with the synoptic estimate of −20 mSv based on shipboard hydrography and absolute geostrophic velocity [*Våge et al.*, 2013]. The monthly mean FWT of the shelfbreak EGC based on the mooring data during these same 2 months were −94 mSv and −55 mSv, while the FWT on the shelf based on the regression with KGA12 were −17 mSv and −18 mSv, respectively. The sum of the shelfbreak and shelf estimates are thus −111 mSV and −73 mSv, which are slightly larger than the −100 mSv and −72 mSv based on the synoptic sections during those months. The main difference between these two sets of

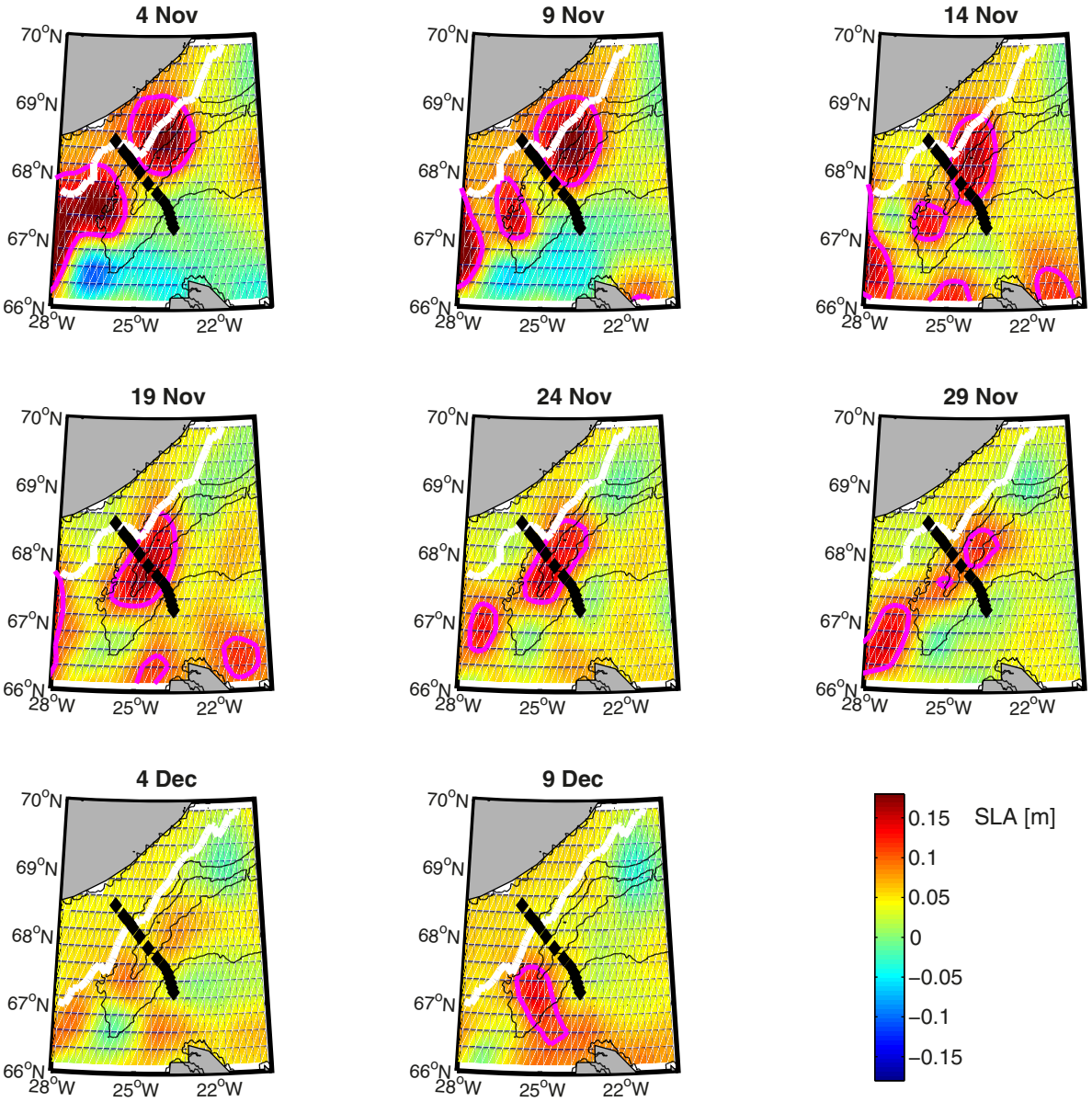

Figure 11. Plots of Sea-Level Anomaly (SLA) north of Denmark Strait shown every 5 days between 4 November and 9 December 2011. The 0.1 m SLA value is marked by the magenta contour. The 80% sea ice concentration is given by the white contour. Inshore of that contour the sea ice concentration is higher, offshore it is lower. The Kögur moorings are indicated by the black diamonds.

measurements is the temporal (monthly) averaging in the case of mooring data. However, Figure 7 shows that the monthly mean southward FWTs in September 2011 and July 2012 are larger than the values at the start and the end of the record, which is when the synoptic surveys were carried out (aliased over a span of approximately five days). It should also be noted that small differences in the mooring-based versus shipboard-based estimates arise from differences in the interpolation methods employed.

The annual mean FWT across the Kögur section (assuming a contribution of the shelf of −20 mSv) of −84 mSv between September 2011 and July 2012 is significantly larger than earlier estimates for this section. In particular, the FWT in September 2011 of −131 mSv and July 2012 of −97 mSv (including the shelf) are nearly two to two and a half times as large as the estimates of −43 mSv to −60 mSv in late summer/autumn of 1998 and 1999 [*Dodd et al.*, 2009] and −55 mSv in summer 2004 [*Sutherland and Pickart*, 2008]. Summer tracer data collected on the Kögur section from 2011 to 2013 have shown that a return of Pacific Water occurred in the EGC [*De Steur et al.*, 2015]. The amount of Pacific Water measured during these 3 years

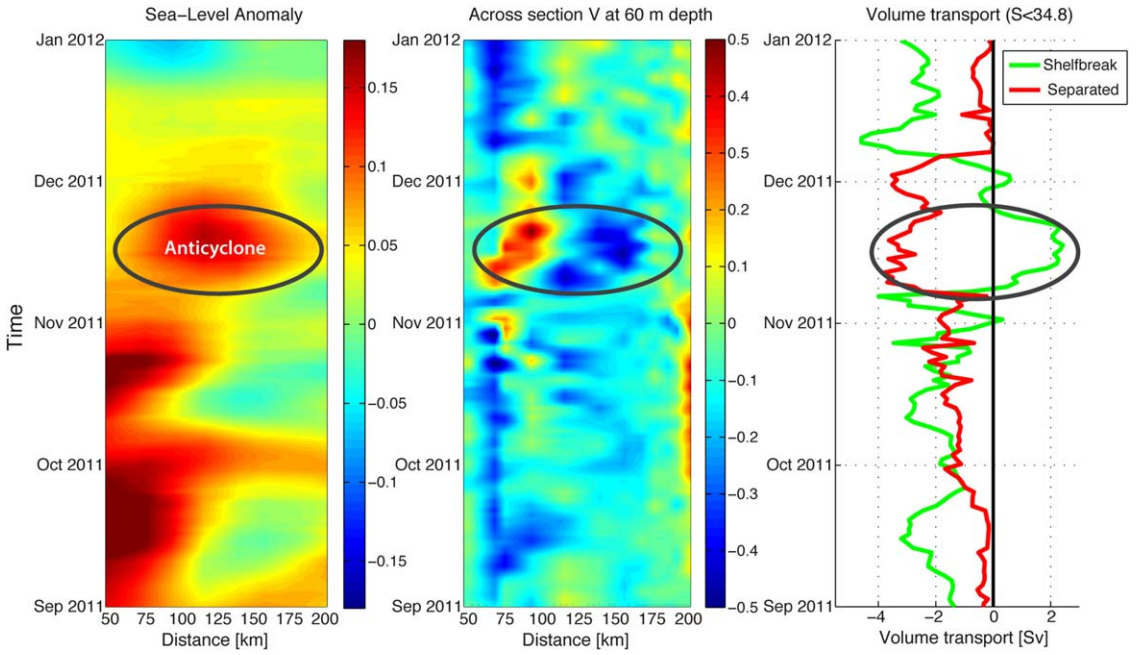

Figure 12. Hovmöller diagrams of (a) Sea-Level Anomaly (SLA) on the mooring section, and (b) across-section velocity at 60 m depth on the mooring section, and (c) volume transports for S<34.8 of the shelfbreak and separated EGC between September 2011 and January 2012. The anticyclone discussed in the text is highlighted.

was comparable to that last seen in the 1990s when a positive NAO was associated with a large efflux of Pacific Water from the Arctic Ocean. This recent increase in Pacific Water, which is typically associated with lower salinities than eastern Arctic freshwater, is likely the reason for the enhanced values of FWT reported here. Moreover, this may have been responsible for elevated FWT during a number of years, i.e., up to 2013.

Another potential source for freshening the Nordic Seas and subpolar Atlantic is discharge from the Greenland Ice Sheet (GIS). Specifically, 2012 was an anomalous year as the entire GIS was melting during the summer [*Tedesco et al*., 2013], hence one wonders if this contributed to the large observed FWT in summer 2012 at the mooring line. The summer mass balance of the GIS in summer 2012 was −627 Gt [*Tedesco et al*., 2013]. Assuming that this was distributed over the different sectors of Greenland in similar fashion as for 1992–2010 (accounting for the increases in different sectors in *Bamber et al*. [2012, Figure 4] relative to 1961–1990), then we find that 11% of the total FW flux from GIS, i.e., 69 Gt, was fluxed into the Nordic Seas in summer 2012. This would be equivalent to 276 km^3yr^{-1} or 9 mSv assuming that the discharge happened during the 3 months of the summer melt season. We note that this is an upper bound of the FWT from GIS into the Nordic Seas since *Tedesco et al*. [2013] also show that most of the anomalous FW in 2012 arrived from the southwestern sector of Greenland. As such, we conclude that the FW contribution from GIS between 2011 and 2012 played only a small role in the FWT in the EGC and cannot account for the observed oceanic increase (approximately 150%) relative to the late 1990s and early 2000s.

The mooring data showed that the FWT and upper ocean volume transport at the Kögur line were significantly modified by the passage of a large anti-cyclone in November 2011, resulting in a temporary flow reversal of the shelfbreak EGC. It is unlikely that such a large feature (order 100 km diameter) was formed via baroclinic instability of the current, which would tend to spawn smaller, deformation-scale eddies (order 25–50 km). The generation of the anti-cyclonic vortex may have been related to the enhanced negative wind-stress curl over the region during October (Figure 10) impacting the shelfbreak EGC upstream of the array. One possibility is that the anomalous southwesterly winds were strong enough to reverse the current, leading to a diversion of water from the shelfbreak to the basin. A cyclonic eddy with negative SLA signature passed the western half of the section in January, which also modified the transports temporarily: the shelfbreak EGC was enhanced while the separated EGC was reversed. The length scale of this feature is more reminiscent of baroclinic instability, suggesting that it was likely a cyclone that was spawned as part of a dipole pair due to instability of the shelfbreak EGC. Such cyclones are found in model shelfbreak jets

[e.g., *Spall et al*., 2008] and are also observed in similar high-latitude boundary current systems (R. Pickart, unpublished data, 2002). A more detailed analysis of such turbulent features north of Denmark Strait is warranted (but beyond the scope of the present study).

The results presented here consider only the liquid FWT at the Kögur section which – including the shelf – amounted to an annual average of −84 mSv. During the summer months in 2011 and 2012 the entire Kögur section was ice free; however, between November and June both the shelf and the shelfbreak EGC are ice covered which contributes significantly to the net freshwater export to the subpolar gyre. A long-term (2000–2008) estimate of sea ice transport in Fram Strait is −66 mSv (for an overview, see *Haine et al*. [2015]), while a similarly long-term (1997–2008) estimate of liquid FWT in the strait is −62 mSv [*De Steur et al*., 2009]. The time series from the mooring array in Fram Strait are presently being updated and new estimates are in preparation for the post-2008 period. Since sea ice thickness has decreased to approximately one third of that in the 1990s [*Hansen et al*., 2013], the total sea ice volume transport has likely decreased as well. At the same time, liquid FWT in Fram Strait may have increased as of 2008 since the Arctic Ocean has freshened during the 2000s [*Proshutinsky et al*., 2009; *McPhee et al*., 2009; *Timmermans et al*., 2011; *De Steur et al*., 2013; *Morison et al*., 2012; *Rabe et al*., 2014]. It is therefore essential to compare the FWT based on data from the mooring array in Fram Strait (updated up to 2013) with the total FWT at the Kögur section between 2011 and 2012. This will help us determine whether a general increase in FWT east of Greenland has taken place, if this was the case for 3 consecutive years (2011–2013), or whether this is related to interannual variability. It will also allow us to estimate the flux of FW into the Greenland and Iceland Seas, which is essential for understanding variations in the freshwater budget of the Nordic Seas and the potential impacts on convection and circulation patterns there. Increased freshwater into the Nordic Seas may impact the formation of dense waters by inhibiting convection or modify density contrasts across the basin with potential impacts on dense water overflows.

5. Conclusions

An 11 month long mooring deployment at the Kögur transect has allowed for a first robust assessment of the liquid FWT north of Denmark Strait. The data indicate that the FWT relative to a salinity of 34.8 of the shelfbreak EGC and separated EGC were roughly −47 mS and −18 mSv, respectively, between August 2011 and July 2012. The FWT estimate for the shelf west of the mooring array was −19 mSv during the year, resulting in a total FWT of −84 ± 30 mSv (standard deviation) across the whole Kögur section. The separated EGC is therefore responsible for nearly 20% of the total FWT across the section, similar to the earlier conclusion of *Våge et al*. [2013] based on four shipboard hydrographic sections. The time series from the mooring array shows a clear seasonal cycle in the FWT. This is primarily due to the reduced FWT in the winter and spring due to higher values of surface salinity (reduced freshwater content). During winter, however, there is a contribution of sea ice to the FWT which has not been incorporated in this analysis. *Aagaard and Carmack* [1989] estimated the FWT related to sea ice near Denmark Strait to be −18 mSv.

The FWT estimate for the Greenland shelf during 2 consecutive years (2012–2013 and 2013–2014) were +1 mSv and −18 mSv respectively. Thus, the transport on the Greenland shelf can be substantial – as much as one third of the total FWT across the section. It is, however, also highly variable. The largest variability occurs in autumn, likely related to synoptic wind forcing such as the strong barrier wind events that occur at this time of the year in this region [*Harden et al*., 2011]. In addition, during late-autumn the sea ice cover is increasing over the shelf. A partial ice cover leads to stronger transfer of momentum to the upper ocean by ocean-ice drag [*Schulze and Pickart*, 2012] and may therefore induce a greater response of the ocean to such wind events. We note that the mooring spacing on the Greenland shelf likely does not fully resolve the spatial variability there (see for instance *Våge et al*. [2013]). This motivates a future deployment of closely-spaced moorings across the shelf, such that the variability can be better resolved and the standard error of the FWT reduced.

Overall, stronger transport of the shelfbreak EGC in winter was associated with a positive wind-stress curl, consistent with what *Harden et al*. [2016] found for the dense overflow water at this location. Notably, the passage of a large mesocale anticyclonic eddy in November induced a large anomalous flow reversal of the shelfbreak EGC and enhanced equatorward transport of the separated EGC. This feature arrived from the shelfbreak north of the Kögur section and passed by the array over a roughly 3 week period. The total

FWT across the section was nearly zero during that time due to the strong northward flow. Roughly a month later a smaller cyclonic eddy caused a temporary increase in the southward transport of the shelf-break EGC and induced northward transport in the separated EGC. Such transient features thus strongly influence the FWT of the boundary current system north of Denmark Strait.

The estimated annual mean FWT from 2011 to 2012 was 70% larger than that obtained from synoptic sections in the late 1990s and in 2004. In particular, the FWT during the summer months was more than twice the earlier estimates from shipboard hydrography/velocity. Together with the return of Pacific Water in the period 2011–2013 north of Denmark Strait, this points to an enhanced FW release from the Arctic in the early 2010s. One explantion could be that the FWT increased temporarily during those years, e.g., through a different atmospheric forcing regime. Alternatively, liquid FWT through Fram Strait may have increased in general relative to earlier years, as a result of ongoing Arctic Ocean freshening.

Acknowledgments
The research leading to these results has received funding from the European Union Seventh Framework Programme (FP7 2007–2013) under grant agreement 308299, NACLIM Project. Additional funding was provided by the US National Science Foundation under grant OCE-0959381. We would like to thank K. Kovacs and C. Lydersen for sharing the hooded seal data that were collected in the Nordic Seas during IPY 2007–2009 at the Norwegian Polar Institute. The NCEP NARR data were provided by the NOAA/OAR/ESRL PSD, Boulder, Colorado, USA, from their web site at http://www.esrl.noaa.gov/psd/. The processed mooring data are available on the website http://www.whoi.edu/science/PO/kogur/php/index.php.

References

Aagaard, K., and E. C. Carmack (1989), The role of sea ice and other fresh water in the Arctic circulation, *J. Geophys. Res.*, *94*(C10), 14,485–14,498.

Bamber, J., M. van den Broeke, J. Ettema, J. Lenaerts, and E. Rignot (2012), Recent large increases in freshwater fluxes from Greenland into the North Atlantic, *Geophys. Res. Lett.*, *39*, L19501, doi:10.1029/2012GL052552.

Cavalieri, D. J., C. L. Parkinson, P. Gloersen, and H. J. Zwally (1996), *Sea Ice Concentrations from Nimbus-7 SMMR and DMSP SSM/I-SSMIS Passive Microwave Data, Version 1*, NASA DAAC at the National Snow and Ice Data Center, Boulder, Colo. [Available at http://dx.doi.org/10.5067/8GQ8LZQVL0VL.]

De Steur, L., E. Hansen, R. Gerdes, M. Karcher, E. Fahrbach, and J. Holfort (2009), Freshwater fluxes in the East Greenland Current: A decade of observations, *Geophys. Res. Lett.*, *36*, L23611, doi:10.1029/2009GL041278.

De Steur, L., et al. (2013), Hydrographic changes in the Lincoln Sea in the Arctic Ocean with focus on an upper ocean freshwater anomaly between 2007 and 2010, *J. Geophys. Res. Oceans*, *118*, 4699–4715, doi:10.1002/jgrc.20341.

De Steur, L., R. S. Pickart, D. K. Torres, and H. Valdimarsson (2015), Recent changes in the freshwater composition east of Greenland, *Geophys. Res. Lett.*, *42*, 2326–2332, doi:10.1002/2014GL062759.

Dickson, R. R., J. Meincke, S.-A. Malmberg, and A. J. Lee (1988), The "great salinity anomaly" in the northern North Atlantic, 1968-1982, *J. Phys. Oceanogr.*, *20*, 103–151.

Dickson, R. R., B. Rudels, S. Dye, M. Karcher, J. Meincke, and I. Yashayaev (2007), Current estimates of freshwater flux through Arctic and subarctic seas, *Prog. Oceanogr.*, *73*, 210–230.

Dodd, P. A., K. J. Heywood, M. P. Meredith, A. C. Naveira-Garabato, A. D. Marca, and K. K. Falkner (2009), Sources and fate of freshwater exported in the East Greenland Current, *Geophys. Res. Lett.*, *36*, L19608, doi:10.1029/2009GL039663.

Dodd, P. A., B. Rabe, E. Hansen, E. Falck, A. Mackensen, E. Rohling, C. Stedmon, and S. Kristiansen (2012), The freshwater composition of the Fram Strait outflow derived from a decade of tracer measurements, *J. Geophys. Res.*, *117*, C11005, doi:10.1029/2012JC008011.

Giles, K. A., S. W. Laxon, A. L. Ridout, D. J. Wingham, and S. Bacon (2012), Western Arctic Ocean freshwater storage increased by wind-driven spin-up of the Beaufort Gyre, *Nat. Geosci.*, *5*, 194–197, doi:10.1038/NGEO1379.

Haine, T. W. N., et al. (2015), Arctic freshwater export: Status, mechanisms, and prospects, *Global Planet. Change*, *125*, 13–35, doi:10.1016/j.gloplacha.2014.11.013.

Hansen, E., S. Gerland, M. A. Granskog, O. Pavlova, A. H. H. Renner, J. Haapala, T. B. Løyning, and M. Tschudi (2013), Thinning of Arctic sea ice observed in Fram Strait: 1990-2011, *J. Geophys. Res. Oceans*, *118*, 5202–5221, doi:10.1002/jgrc.20393.

Harden, B., I. Renfrew, and G. Petersen (2011), A climatology of wintertime barrier winds off southeast Greenland, *J. Clim.*, *24*, 4701–4717, doi:10.1175/2011JCLI4113.1.

Harden, B., et al. (2016), Upstream sources of the Denmark Strait Overflow: Observations from a high-resolution mooring array, *Deep Sea Res., Part I*, *112*, 94–112, doi:10.1016/j.dsr.2016.02.007.

Holfort, J., and J. Meincke (2005), Time series of freshwater-transport on the East Greenland Shelf at 74°N, *Meteorol. Z.*, *14*(6), 703–710.

Isachsen, P. E., S. Sørlie, C. Mauritzen, C. Lydersen, P. Dodd, and K. Covacs (2014), Upper-ocean hydrography of the Nordic Seas during the International Polar Year (2007-2008) as observed by instrumented seals and Argo floats, *Deep Sea. Res., Part I*, *93*, 41–59, doi:10.1016/j.dsr.2014.06.012.

Jahn, A., et al. (2012), Arctic Ocean freshwater: How robust are model simulations?, *J. Geophys. Res.*, *117*,C00D16, doi:10.1029/2012JC007907.

Jónsson, S., and H. Valdimarsson (2004), A new path for the Denmark Strait overflow water from the Iceland Sea to Denmark Strait, *Geophys. Res. Lett.*, *31*, L03305, doi:10.1029/2003GL019214.

Karcher, M., R. Gerdes, F. Kauker, C. Köberle, and I. Yashayaev (2005), Arctic Ocean change heralds North Atlantic freshening, *Geophys. Res. Lett.*, *32*, L21606, doi:10.1029/2005GL023861.

Macrander, A., H. Valdimarsson, and S. Jónsson (2014), Improved transport estimate of the East Icelandic Current 2002–2012, *J. Geophys. Res. Oceans*, *119*, 3407–3424, doi:10.1002/2013JC009517.

Manabe, S., and R. J. Stouffer (1995), Simulation of abrupt climate change induced by freshwater input to the North Atlantic Ocean, *Nature*, *378*, 165–167.

McPhee, M. G., A. Proshutinsky, J. H. Morison, M. Steele, and M. B. Alkire (2009), Rapid change in freshwater content of the Arctic Ocean, *Geophys. Res. Lett.*, *36*, L10602, doi:10.1029/2009GL037525.

Mesinger, F., G. DiMego, E. Kalnay, K. Mitchell, and P. Shafran (2006), North American Regional Reanalysis, *Bull. Am. Meteorol. Soc.*, *87*, 343–360.

Morison, J., R. Kwok, C. P. Peralta-Ferritz, M. Alkire, I. Rigor, R. Andersen, and M. Steele (2012), Changing Arctic Ocean freshwater pathways, *Nature*, *481*, 66–70, doi:10.1038/nature10705.

Nilsson, J., G. Björk, B. Rudels, P. Winsor, and D. Torres (2008), Liquid freshwater transport and Polar Surface Water characteristics in the East Greenland Current during the AO-02 Oden expedition, *Prog. Oceanogr.*, *78*, 45–57, doi:10.1016/j.pocean.2007.06.002.

Pickart, R. S., M. A. Spall, and J. T. Mathis (2013), Dynamics of upwelling in the Alaskan Beaufort Sea and associated shelfbasin fluxes, *Deep Sea Res., Part I*, *76*, 106–122, doi:10.1016/j.dsr.2013.01.007.

Proshutinsky, A., R. Krishfield, M.-L. Timmermans, J. Toole, E. Carmack, F. A. McLaughlin, W. J. Williams, S. Zimmerman, M. Itoh, and K. Shimada (2009), The Beaufort Gyre freshwater reservoir: State and variability from observations, *J. Geophys. Res.*, *114*, C00A10, doi:10.1029/2008JC005104.

Rabe, B., M. Karcher, F. Kauker, U. Schauer, J. Toole, R. A. Krishfield, S. Pisarev, T. Kikuchi, and J. Su (2014), Arctic Ocean basin liquid freshwater storage trend 1992–2012, *Geophys. Res. Lett.*, *41*, 961–968, doi:10.1002/2013GL058121.

Schulze, L. M., and R. S. Pickart (2012), Seasonal variation of upwelling in the Alaskan Beaufort Sea: Impact of sea ice cover, *J. Geophys. Res.*, *117*, C06022, doi:10.1029/2012JC007985.

Spall, M. A., R. S. Pickart, P. Fratantoni, and A. Plueddemann (2008), Western Arctic Shelfbreak Eddies: Formation and transport, *J. Phys. Oceanogr.*, *38*, 1644–1668.

Sutherland, D. A., and R. S. Pickart (2008), The East Greenland Coastal Current: Structure, variability, and forcing, *Prog. Oceanogr.*, *78*, 58–77, doi:10.1016/j.pocean.2007.09.006.

Tedesco, M., X. Fettweis, T. Mote, J. Wahr, P. Alexander, J. Box, and B. Wouters (2013), Evidence and analysis of 2012 Greenland records from spaceborne observations, a regional climate model and reanalysis data, *Cryosphere*, *7*, 615–630, doi:10.5194/tc-7-615−2013.

Timmermans, M.-L., A. Proshutinsky, R. A. Krishfield, D. K. Perovich, J. A. Richter-Menge, T. P. Stanton, and J. M. Toole (2011), Surface freshening in the Arctic Ocean's Eurasian Basin: An apparent consequence of recent change in the wind-driven circulation, *J. Geophys. Res.*, *116*, C00D03, doi:10.1029/2011JC006975.

Våge, K., R. S. Pickart, M. A. Spall, G. Moore, H. Valdimarsson, D. J. Torres, S. Y. Erofeeva, and J. E. Ø. Nilsen (2013), Revised circulation scheme north of the Denmark Strait, *Deep Sea Res., Part I*, *79*, 20 – 39, doi:10.1016/j.dsr.2013.05.007.

Yamamoto-Kawai, M., F. A. McLaughlin, E. C. Carmack, S. Nishino, K. Shimada, and N. Kurita (2009), Surface freshening of the Canada Basin, 2003-2007: River runoff versus sea ice meltwater, *J. Geophys. Res.*, *114*, C00A05, doi:10.1029/2008JC005000.